Energetic Materials Frontiers xxx (xxxx) xxx

Contents lists available at ScienceDirect

Energetic Materials Frontiers

journal homepage: www.keaipublishing.com/en/journals/energetic-materials-frontiers

Development of an infrared laser absorption sensor for non-intrusive gas temperature measurements

Kun Duan [a,1], Da-xin Wen [a,b,1], Yu Wang [b], Liu-hao Ma [a,b,*], Kin-Pang Cheong [c], Chao-kai Yuan [d], Wei Ren [a]

[a] Department of Mechanical and Automation Engineering, The Chinese University of Hong Kong, New Territories, Hong Kong SAR, China
[b] Laboratory for Advanced Combustion, School of Automotive Engineering, Wuhan University of Technology, Wuhan, 430081, China
[c] School of Aeronautics and Astronautics, Sichuan University, Chengdu, 610065, China
[d] State Key Laboratory of High Temperature Gas Dynamics, Institute of Mechanics, Chinese Academy of Sciences, Beijing, 100190, China

ARTICLE INFO

Keywords:
Laser absorption sensor
High temperature
Benchmark laminar premixed flame
Numerical simulation

ABSTRACT

Energetic materials have extremely high volumetric and specific energy densities, making them attractive and important in combustion systems. To improve their combustion performance, reliable temperature acquirement method is highly demanded. A laser sensor was developed for *in situ* and quantitative measurements of gas temperature. Scanned-wavelength direct absorption spectroscopy was used for line-of-sight temperature measurements. Multiple H_2O absorption features in the near-infrared combination band ($\nu_1+\nu_3$) and mid-infrared fundamental band (ν_3) were selected to establish four absorption line pairs with good temperature sensitivity. Three infrared distributed feedback lasers (DFB) were used to cover the selected absorption lines. The accuracy and uncertainty of the sensor were first numerically evaluated in a wide temperature range of 1000–3000 K under different Gaussian white noise levels (5–20%). A free-space optical setup was established to experimentally evaluate the sensor performance by measuring benchmark laminar premixed flames, which were compared with additional thermocouple measurements, chemical kinetic modeling and computational fluid dynamics simulations. The good performance of the current sensor indicates the potential of being used in non-intrusive, *in-situ* and quantitative diagnostics of the energetic materials combustion.

1. Introduction

Energetic materials have been widely used as additives and fuels in combustion and propulsion systems.[1] Accurate knowledge of the combustion properties of energetic materials is crucial to fundamental chemical kinetics and development of novel propellants and explosives. Although many efforts have been dedicated to modeling, the experimental study still attracts considerable attention.[2,3] Among various thermochemical parameters relevant to the combustion of energetic materials, the temperature is a key parameter that determines chemical reaction rates and reflects important combustion processes such as ignition, blow-off and instability. However, temperature measurement in energetic material combustion is challenging due to its highly transient and multi-phase nature. In addition, the traditional thermocouple method is no longer applicable in the presence of high temperature (above the melting point of the Pt/Rh material), particle deposition and intrusive disturbance to the local combustion field.

Optical diagnostic techniques can provide non-intrusive measurements with a high sensitivity and a wide temperature range.[4] Passive emission spectroscopy and active laser-based techniques are two typical methods used for temperature sensing. Emission spectroscopy utilizes the two-color or multi-color emissions collected from high-temperature particles to infer temperature.[5] This method is usually realized by a combination of a CCD camera and multiple bandpass filters, which requires frequent calibrations and sophisticated mathematical models to process the raw images. Laser-based methods obtain temperature from various spectroscopic information including absorption,[6] dispersion,[7] fluorescence[8] or scattering[9–11] process when the laser beam interacts with the relevant molecules, atoms or radicals in the combustion field. Among different laser-based techniques, laser-absorption spectroscopy

* Corresponding author. Laboratory for Advanced Combustion, School of Automotive Engineering, Wuhan University of Technology, Wuhan, 430081, China.
E-mail address: liuhaoma@whut.edu.cn (L.-h. Ma).
[1] The authors contribute equally.

https://doi.org/10.1016/j.enmf.2021.10.003
Received 3 September 2021; Received in revised form 30 September 2021; Accepted 2 October 2021
Available online xxxx
2666-6472/© 2021 The Authors. Publishing services by Elsevier B.V. on behalf of KeAi Communications Co. Ltd. This is an open access article under the CC BY-NC-ND license (http://creativecommons.org/licenses/by-nc-nd/4.0/).

Please cite this article as: Duan K et al., Development of an infrared laser absorption sensor for non-intrusive gas temperature measurements, Energetic Materials Frontiers , https://doi.org/10.1016/j.enmf.2021.10.003

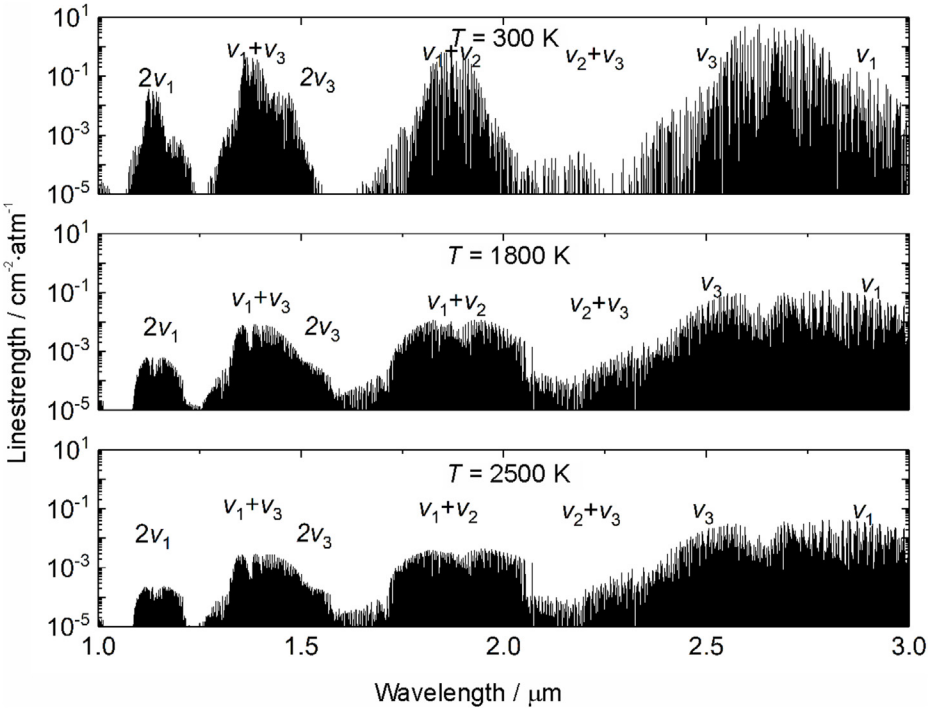

Fig. 1. Line-strength of H_2O at 300 K, 1800 K and 2500 K in the spectral range of 1–3 μm based on the HITRAN database.[20]

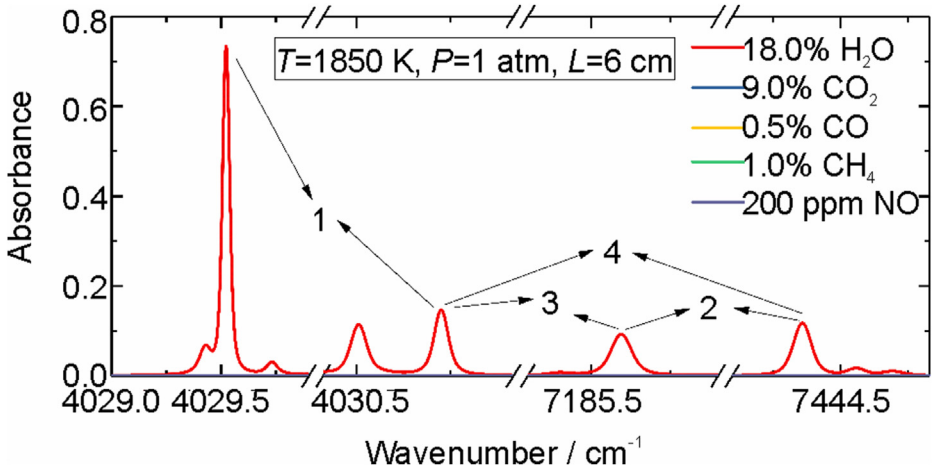

Fig. 2. Simulated absorption features of the selected lines near 1343 nm, 1392 nm and 2482 nm under typical benchmark laminar premixed flame conditions: $T = 1850$ K, $P = 1$ atm, $X_{H_2O} = 18.0\%$, $X_{CO_2} = 9.0\%$, $X_{CO} = 0.5\%$, $X_{CH_4} = 1.0\%$, $X_{NO} = 200$ ppm.

Table 1
Spectroscopic parameters of the selected line pairs.[20]

Line Pair	Frequency/ cm^{-1}	Wavelength/ nm	S(296K)/ $cm^{-2}atm^{-1}$	E''/cm^{-1}	$\triangle E''$/ cm^{-1}
1	4029.52	2481.69	1.10×10^{-4}	2660.95	2228.54
	4030.73	2480.94	2.68×10^{-9}	4889.49	
2	7185.60	1391.67	1.96×10^{-2}	1045.06	729.69
	7444.35/ 7444.37	1343.30	1.12×10^{-3}	1774.75/ 1806.67	
3	4030.73	2480.94	2.68×10^{-4}	4889.49	3844.43
	7185.60	1391.67	1.96×10^{-2}	1045.06	
4	4030.73	2480.94	2.68×10^{-4}	4889.49	3114.74
	7444.35/ 7444.37	1343.30	1.12×10^{-3}	1774.75/ 1806.67	

(LAS) is the most representative one as it provides *in situ*, sensitive, calibration-free and quantitative measurements of multiple combustion parameters with a simple optical setup and signal processing.[12]

LAS has been widely used in lab-scale burners, shock tubes, and practical combustion systems in the past decade.[12] Various measurement strategies have been developed to extend the technique to harsh measurement environments,[13] to quantitatively determine the thermochemical non-uniformity,[14] to reconstruct the fine thermochemical image,[15] and to enhance the temperature sensitivity.[16] In order to further extend the temperature measurement sensitivity and range, a cross-band thermometry has been proposed and successfully used in shock tube and flame measurements.[16–18]

In this work, an infrared laser sensor was developed for *in situ* and quantitative high-temperature measurements. Four H_2O absorption

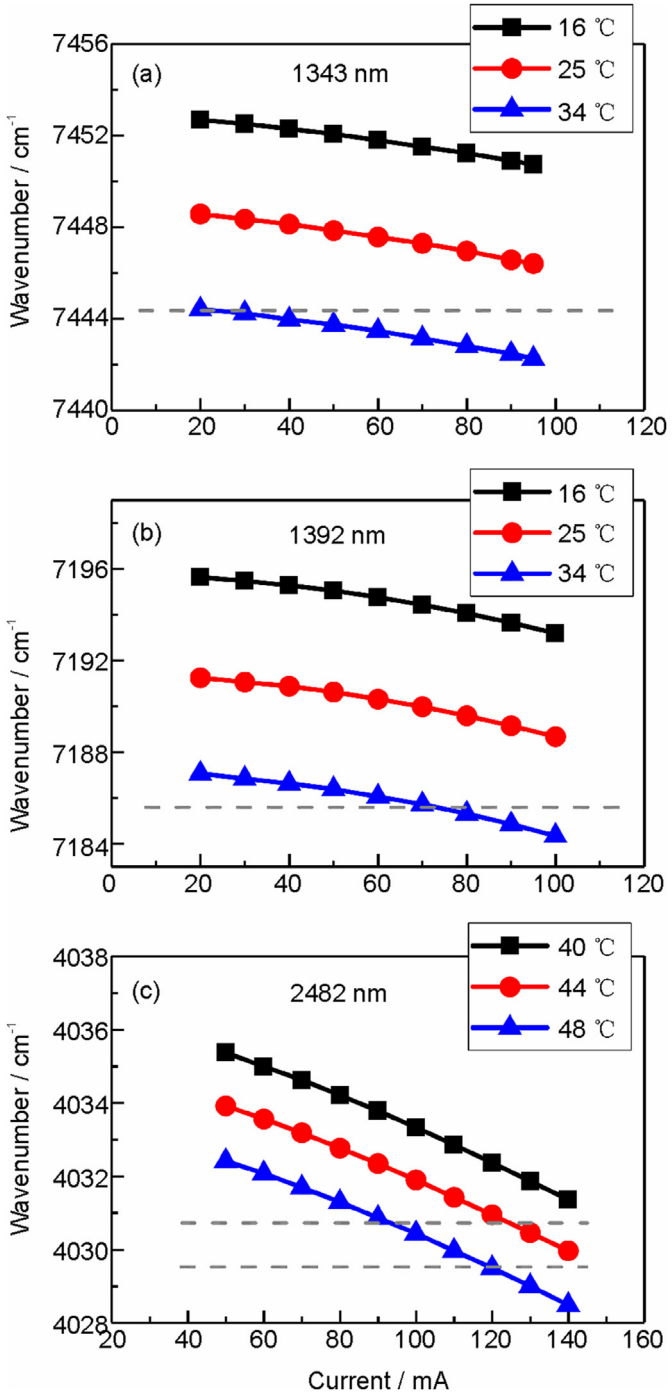

Fig. 3. Characterization of the wavelength tuning performance of the three DFB lasers: (a) 1343 nm, (b) 1392 nm, (c) 2482 nm.

transitions near 1343 nm, 1392 nm and 2482 nm were selected to establish four line pairs for two-line thermometry development. The sensor performance was firstly numerically evaluated for the selected line pairs, and a good agreement was found between the best-fit temperature and the set value. Then the sensor capability was examined by measuring benchmark laminar premixed flames with the results compared to thermocouple measurements, chemical kinetic modeling and computational fluid dynamics simulations. The non-monotonic variation of temperature was successfully captured and the measurement uncertainty was mostly within 80 K. By combining with the temperature-binning strategy, the possibility of using the sensor for non-uniform temperature distribution is also discussed.

2. Spectroscopic fundamentals

The spectroscopic fundamentals of laser absorption spectroscopy (LAS) for temperature sensing have been well documented in the literature.[19] In this section, a brief review of the spectroscopic principles and measurement strategies is presented to clarify the relevant definition and nomenclature. LAS exploits the resonance of atoms, molecules or radicals to determine the thermochemical parameters of the combustion field from the attenuated laser intensity. When a laser beam at a specific optical frequency ν [cm^{-1}] passes through a uniform absorbing gas sample with a total length of L, the ratio of transmitted laser intensity (I_t) and incident laser intensity (I_0) is governed by the well-known Beer-Lambert law[19]:

$$\alpha_\nu = -\ln\left(\frac{I_t}{I_0}\right) = S_i(T)PX_{abs}L\varphi_\nu \tag{1}$$

where α_ν denotes the spectral absorbance, P [atm] represents the total gas pressure; $S_i(T)$ [cm^{-2} atm^{-1}] is the line-strength of the specific transition i, which is only a function of temperature; T [K] and X_{abs} represent the temperature and absorbing species concentration; and φ_ν [cm] is the line-shape function. The temperature-dependent line-strength $S_i(T)$ is defined as:

$$S_i(T) = S_i(T_0)\frac{Q(T_0)}{Q(T)}\frac{T_0}{T}\exp\left[-\frac{hcE_i''}{k}\left(\frac{1}{T}-\frac{1}{T_0}\right)\right]\left[\frac{1-\exp(-hc\nu_{0i}/kT)}{1-\exp(-hc\nu_{0i}/kT_0)}\right] \tag{2}$$

where h [J·s], c [cm·s^{-1}] and k [J·K^{-1}] are the Planck's constant, speed of light and Boltzmann constant, respectively; ν_0 indicates the line center frequency of the absorption transition, $S(T_0)$ represents the line-strength at the reference temperature T_0 (296 K), E_i'' denotes the lower state energy of the transition, and $Q(T)$ is the partition function of the absorption species. Both $S(T_0)$ and temperature-dependent $Q(T)$ are listed in the HITRAN[20] or HITEMP database.[21]

It should be noted that φ_ν is a normalized function such that $\int_{-\infty}^{\infty}\varphi_\nu d\nu \equiv 1$ and the line-shape is typically modeled using the Voigt function[22] to include the Doppler-broadening and collisional-broadening effects.[23] In the numerical and experimental part of this work, the Voigt function is used to simulate the absorption features at different temperatures and to fit the measured absorption profiles. Hence, the spectrally integrated absorbance (A_i) over the entire frequency can be expressed by the following equation:

$$A_i = \int_{-\infty}^{\infty}\alpha_\nu d\nu = S_i(T)PX_{abs}L \tag{3}$$

If two different absorption lines are experimentally measured, temperature can be derived from the ratio of two integrated absorbances ($R = A_1/A_2$) and Equation (2). The final expression of the derived temperature can be expressed as follows:

$$T = \frac{\frac{hc}{k}\left(E_2''-E_1''\right)}{\ln(R)+\ln\left(\frac{S_2(T_0)}{S_1(T_0)}\right)+\frac{hc}{k}\frac{\left(E_2''-E_1''\right)}{T_0}} \tag{4}$$

The aforementioned method is known as two-line thermometry. The optimal selection of absorption lines is important to ensure reliable, sensitive and accurate measurements. The golden standard for line selection includes good spectral isolation, sufficiently large line-strength, and enough temperature sensitivity.[24] As H_2O is one of the major products of many reaction systems, Fig. 1 presents the line-strength of H_2O at different temperatures within the spectral range of 1–3 μm, which can be accessed by commercially available distributed feedback diode lasers. For high-temperature sensing purposes, most of previous well-validated high-temperature sensors were developed using the intra-band line pairs near 1.4 μm,[25–27] 1.8 μm,[28] 2.5 μm[29-31] and 2.9 μm.[32]

In this work, four absorption lines at 4029.52 cm^{-1}, 4030.73 cm^{-1}, 7185.60 cm^{-1} and 7444.36 cm^{-1} are selected in the mid-infrared

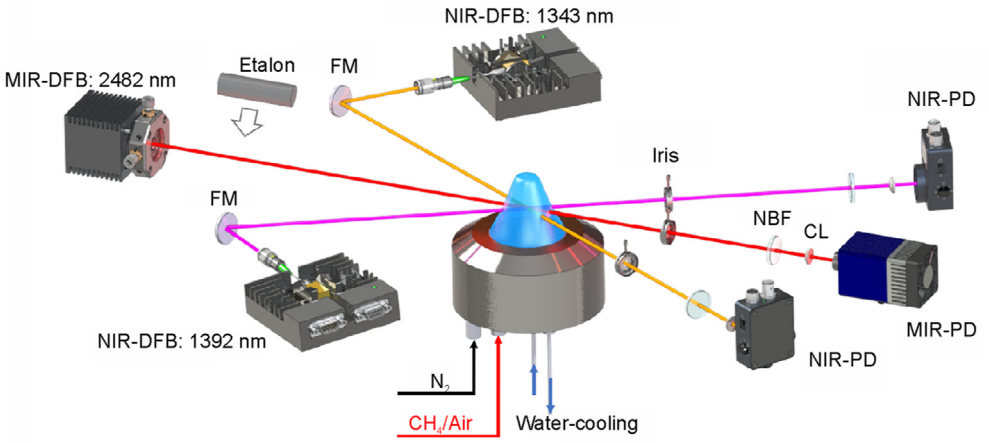

Fig. 4. Experimental setup of the laser absorption sensor. DFB, distributed feedback diode laser; PD, photodetector; DM, dichroic mirror; BS, beamsplitter; NBF, narrow-band-pass filter; CL, convex lens.

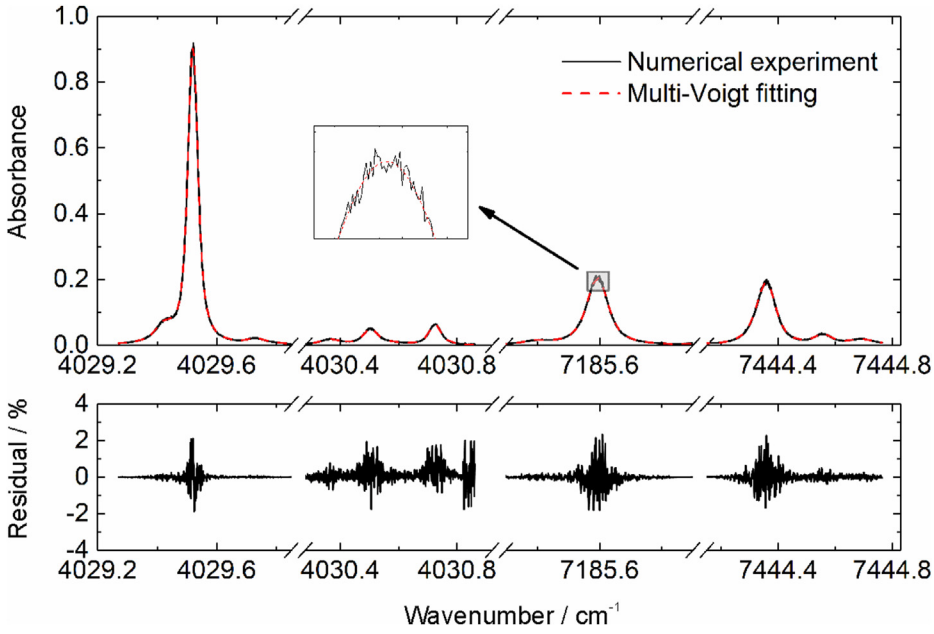

Fig. 5. Typical Voigt-fitting results of simulated absorbance with 5% noise added, along with the fitting residuals (bottom panel).

fundamental band (ν_3) and near-infrared combination band ($\nu_1+\nu_3$). As illustrated in Fig. 2, these lines are well isolated from other major, intermediate and minor species (e.g., CO_2, CO, CH_4, NO). The peak absorbance is larger than 0.01 under the typical condition of benchmark laminar premixed flame. The selected four absorption lines are then used to establish four line pairs, including two intra-band line pairs and two cross-band line pairs. The spectroscopic parameters of these line pairs are listed in Table 1.

3. Laser characterization

The wavelength tuning performance of the three continuous-wave (CW) DFB lasers was characterized using infrared spectral analyzers (Yokogawa, AQ6370, and Bristol Instruments, 771B). Fig. 3 presents the calibrated wavelength as a function of the injection current at different operating temperatures. By fixing the operating temperature at a certain value, these lasers can be readily tunned to cover the desired absorption lines using a single scan of the injection current. As illustrated in Fig. 3, the horizontal dash lined indicates the wavelength of the selected absorption line.

4. Experimental

In this work laminar CH_4/air premixed flames were selected to validate the sensor performance. The selected laminar flames were generated in a McKenna burner with an inner plug diameter of 60 mm. The flow rates of fuel, oxidizer and co-flow nitrogen were precisely monitored by mass flow controllers (MFC, Sevenstars, ±1% precision). Before optical measurements, the MFCs were warmed up for half an hour to ensure stable monitoring. Flame conditions were varied ($\Phi = 0.8$ - 1.2) by adjusting the airflow rates when the flow rate of CH_4 was fixed at 1.5 L min^{-1}. For demonstration purposes, all the measurements were performed at the height of 5 mm above the burner surface.

The schematic of the experimental setup is depicted in Fig. 4. A mid-infrared DFB laser near 2.5 μm and two near-infrared DFB lasers near 1.4 μm were used as light sources to cover the selected absorption features. Temperature and injection current of the DFB lasers were controlled by low-noise laser drivers (Wavelength Electronics, LDTC0520). The DFB lasers were tuned by triangle signals at 100 Hz, produced by a function generator (Tektronix, AFG3052C). For each optical path, the incident

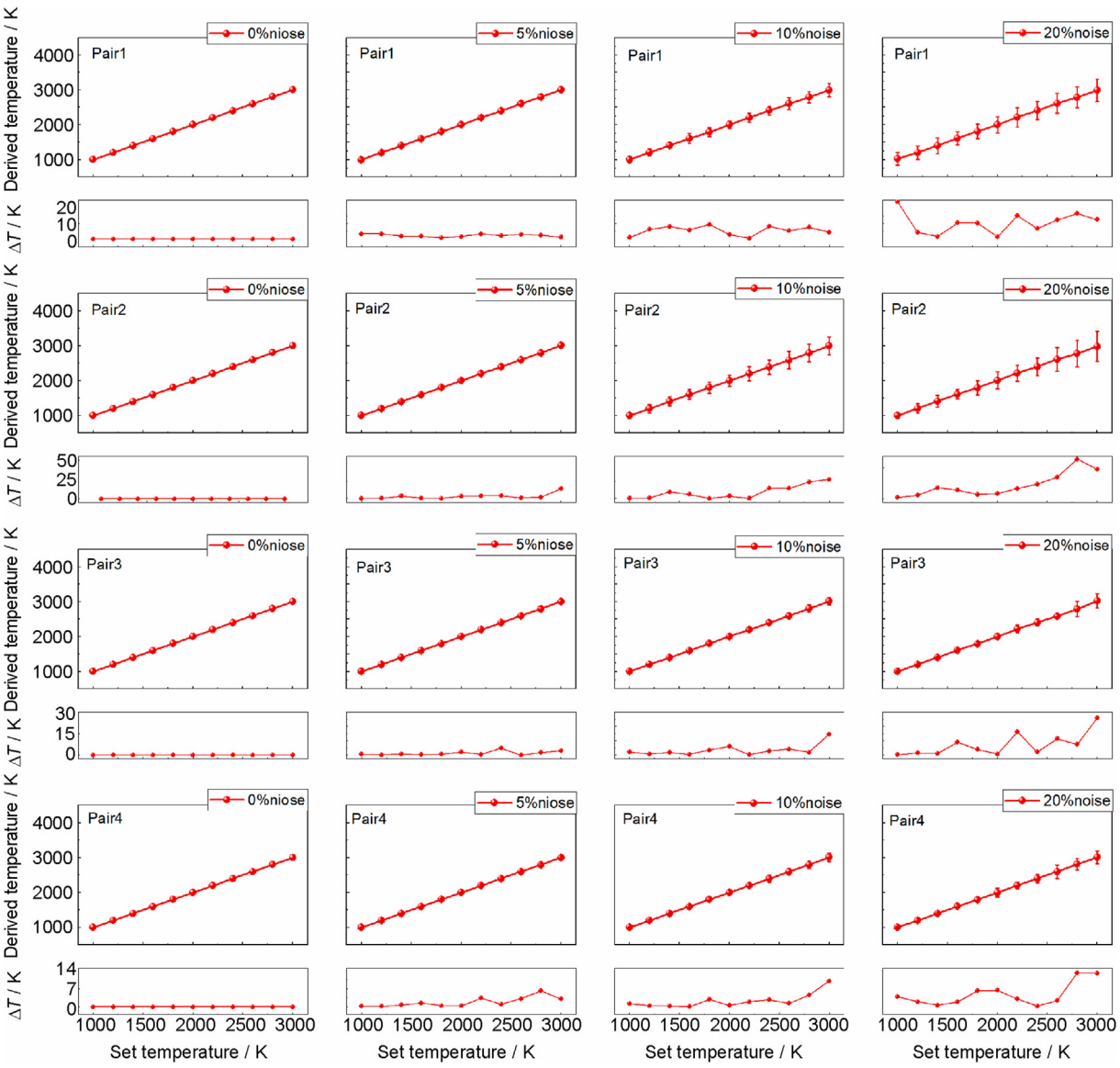

Fig. 6. Comparison of the derived temperature and the set temperature. The absolute temperature difference is plotted in the bottom panel.

laser beam was directed through the flame center and the transmitted laser beam was then collected by a photodetector using a convex lens. In addition, a narrowband optical filter and an iris were placed before the photodetector to eliminate most of the background thermal radiation. Besides, an etalon was utilized for calibration of the relative wavelength.

5. Results and discussion

5.1. Numerical simulation

The computational modeling analysis of the optical thermometry was firstly performed to evaluate the measurement accuracy and uncertainty under different noise levels. The Gaussian white noise was used with the noise level set to be 5–20% over the temperature range of 1000–3000 K. The numerical simulation process can be described as follows. Firstly, thermochemical parameters (e.g., temperature, gas concentration and pressure), optical path length and spectroscopic parameters are the initial input parameters for the spectral simulation. Noise levels are then added to the simulated spectral features. By applying the non-linear spectral fitting to the simulated absorption profile, the integrated absorbance can be obtained to derive the temperature using Equation (4).

Fig. 5 shows the typical multi-line Voigt-fitting results of the simulated absorbance with 5% Gaussian white noise and the relevant fitting residuals are shown in the bottom panel. The enlarged figure illustrates the detail of noise added absorbance. For the selected lines, fitting residuals less than 3% were observed under 5% Gaussian white noise.

Fig. 6 depicts the set temperature and the derived temperature for the selected four absorption line pairs under different noise levels. The error bars indicate the uncertainty of the derived temperature and the bottom panel represents the absolute temperature differences (ΔT) between the derived temperature and set temperature. Every derived temperature shown here was the averaged value of 50 times independent spectra fitting derived temperature. The uncertainty source came from the fitting error to the simulated absorption profile and the variation of the derived temperature during 50 independent numerical experiments. Meanwhile line pair 2 shown larger uncertainty under larger added noise level among the four line pairs, due to its smallest difference of E''. The uncertainties were estimated by considering the type A uncertainty determined by the statistic of repeated measurements and the uncertainty determined by spectroscopic parameters and integrated absorbance, which is detailed in literature.[33] Over the temperature of 1000–3000 K, the derived temperature was in excellent agreement with the set

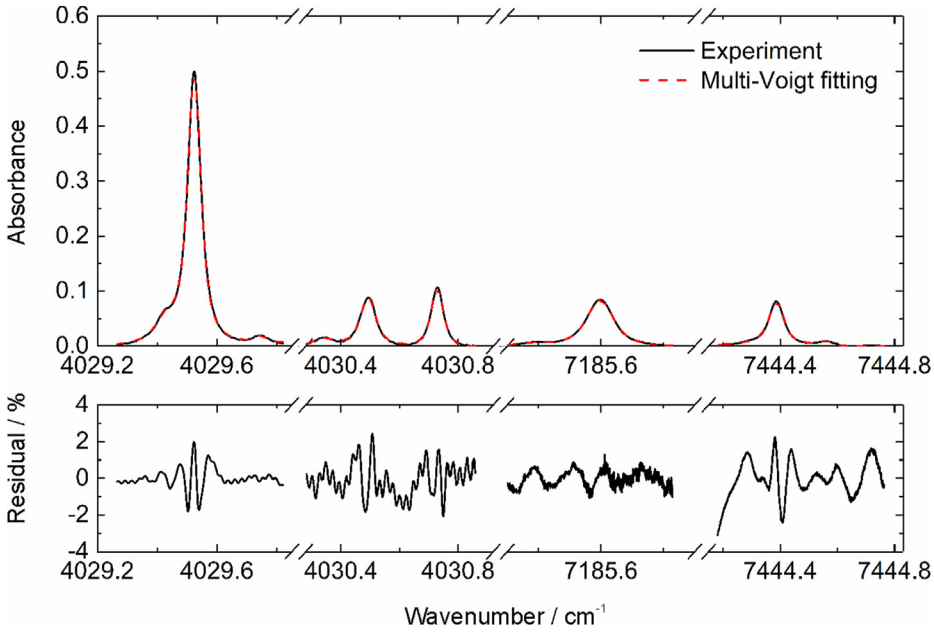

Fig. 7. Typical measured absorption spectra along with the Voigt-fitting and fitting residuals for laminar CH_4/air premixed flame at the stoichiometric condition.

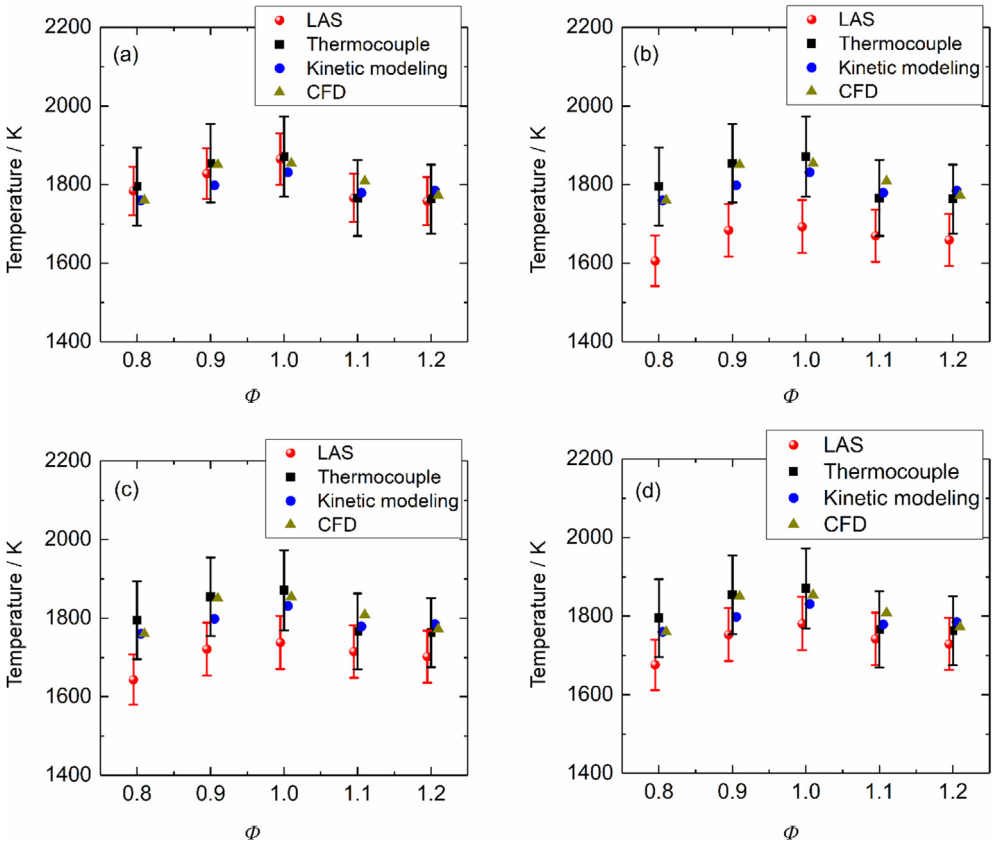

Fig. 8. Measured temperature at different equivalence ratios using (a) line pair 1, (b) line pair 2, (c) line pair 3, (d) line pair 4.

temperature when the noise level varies from 5% to 20%. For each line pair, the ΔT was observed to increase with the noise level, and the maximum ΔT for line pairs 1, 2, 3 and 4 were 25 K, 51 K, 26 K and 26 K, respectively. In addition, the temperature derived from the spectral average was close to the set true temperature, indicating the unwanted noise can be eliminated by signal averaging.

5.2. Experimental results

The thermochemical non-uniformity exists in the standard premixed flame burner, which may affect the measured absorption spectra due to the non-linear effect of line-strength and line-shape function. These effects make it more difficult in the subsequent spectral fitting. It is

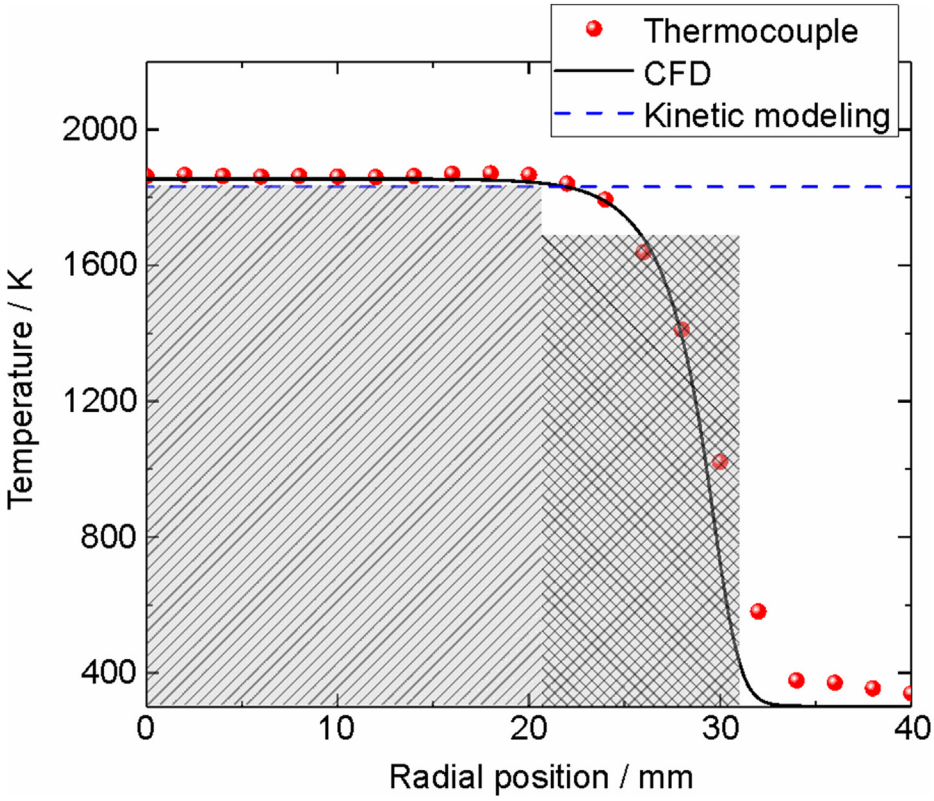

Fig. 9. Radial distribution of temperature at 5 mm above the burner surface for $\Phi = 1.0$. The shaded regions indicate the LAS-determined result using the temperature-binning strategy.

necessary to optimize the spectral fitting process to obtain the accurate path-integrated spectrum. During the spectral fitting process, the integrated area and collisional width are two variables while the Doppler width is an estimated value. This estimation was determined to have a negligible effect on the derived integrated absorbance.

Additionally, at relatively high temperatures, the targeted H_2O absorption transitions may be partially blended with nearby transitions. Hence, the multi-line Voigt-fitting method is needed to account for the possible overlapping issue of absorption features. Fig. 7 depicts the typical absorption profiles of the selected spectral features along with the spectral-fitting results. Each experiment absorbance was shown as the result of 10 times measurement averaging. The fitting residual was observed to be mostly within 2%, and such a small residual enables an accurate determination of the integrated absorbance.

Fig. 8 shows the measured temperature at different equivalence ratios (Φ = 0.8–1.2). Note that the traditional thermocouple measurement, chemical kinetic modeling and computational fluid dynamics (CFD) simulation are provided for comprehensive comparisons. Further details of the simulation and modeling are referred to our previous work.[30,34] In general, the non-monotonic variation of temperature was successfully captured by all the four line pairs. The measurement uncertainty was mostly within about 80 K. The maximum uncertainty occurs in the measurements using line pair 2, which is due to the relatively large fitting residual. Different discrepancies between measured temperature from LAS and other methods were observed for four line pairs, which is caused by the thermochemical non-uniformity, non-linearly temperature-dependent line-strength and line-pairs lower state energy difference.[35] For line pair 1, a good agreement was found between the LAS-measured temperature and reference temperature, where the temperature difference was mostly within 40 K. However, since the lower state energy difference of line pair 2 is not large enough, which makes them sensitive to the thermochemical non-uniformity, an evident temperature difference was found using line pair 2. Regarding the measurements using line pairs 3 and 4, a similar discrepancy between the LAS-measured temperature and reference temperature data was observed. However, such a discrepancy is smaller compared to that observed by line pair 2, which is mainly because of the larger values of the lower state energy for line pairs 3 and 4.

In the presence of flame thermochemical gradient, the temperature-binning strategy[36] is an effective method to resolve the non-uniform distribution. As only four absorption features were simultaneously measured in this work, the absorption path was discretized into two regions. Fig. 9 compares the temperature binning result with the reference temperature at Φ = 1.0. The central temperature was well predicted by the first bin. However, the second bin lost fidelity, which is limited by the number of absorption features. Once more absorption features are accessed and more bins are discretized, the results will be fine enough to resolve the radial distribution.

6. Conclusions

We reported the development of a two-line infrared laser absorption sensor for quantitative measurements of high temperature flows. Four H_2O absorption line pairs were selected for sensitive temperature measurements, including intra-band mid-infrared line pair, intra-band near-infrared line pair and cross-band line pairs. The sensor performance was firstly evaluated within 1000–3000 K under different noise levels (5–20%) by the numerical analysis. Among the selected line pairs, a good agreement was found between the derived temperature and the set temperature. Successful measurements in benchmark laminar premixed flames further demonstrated the feasibility of the sensor for high-temperature measurements. Future work will involve the improvement of the time response for highly-transient ignition processes of energetic materials and the fundamental study of energetic materials combustion.

Conflicts of interest

The authors have no conflicts to declare.

Acknowledgments

This work was supported by National Natural Science Foundation of China (52106221, 52006152, 51976142, 51776179), Fundamental Research Funds for the Central Universities (WUT:2021IVA016), Startup funding of Wuhan University of Technology (40120607), Open Funding from State Key Laboratory of High-temperature Gas Dynamics, Science Foundation of Sichuan Province (No. 2020JDRC0034) and Research Funding from Department of Kitchen and Heat Water in Midea. Dr. Liuhao Ma also acknowledges the technical assistance from Mr. Gang Sheng and Mr. Wei Wang.

References

1. Shang Y, Wang Z, Ma L, et al. Shock tube measurement of NO time-histories in nitromethane pyrolysis using a quantum cascade laser at 5.26 μm. *Proc Combust Inst.* 2021;38(1):1745–1752.
2. Ruesch MD, McDonald AJ, Mathews GC, Son SF, Goldenstein CS. Characterization of the influence of aluminum particle size on the temperature of composite-propellant flames using CO absorption and AlO emission spectroscopy. *Proc Combust Inst.* 2021;38(3):4365–4372.
3. Shang Y-l, Li C, He L, et al. Ignition characteristics of nitromethane-doped ethanol in a heated shock tube. *Energ Mater Front.* 2021;2(3):174–180.
4. Hanson RK, Davidson DF. Recent advances in laser absorption and shock tube methods for studies of combustion chemistry. *Prog Energy Combust Sci.* 2014;44:103–114.
5. Li K, Yan W, Huang X, Yu L, Chen Y, Lou C. In-situ measurement of temperature and potassium concentration during the combustion of biomass pellets based on the emission spectrum. *Fuel.* 2021:289.
6. Hanson RK. Applications of quantitative laser sensors to kinetics, propulsion and practical energy systems. *Proc Combust Inst.* 2011;33(1):1–40.
7. Ma L, Wang Z, Cheong K-P, Ning H, Ren W. Mid-infrared heterodyne phase-sensitive dispersion spectroscopy in flame measurements. *Proc Combust Inst.* 2019;37(2):1329–1336.
8. Schulz C, Sick V. Tracer-LIF diagnostics: quantitative measurement of fuel concentration, temperature and fuel/air ratio in practical combustion systems. *Prog Energy Combust Sci.* 2005;31(1):75–121.
9. Roy S, Gord JR, Patnaik AK. Recent advances in coherent anti-Stokes Raman scattering spectroscopy: fundamental developments and applications in reacting flows. *Prog Energy Combust Sci.* 2010;36(2):280–306.
10. Zhao F-Q, Hiroyasu H. The applications of laser Rayleigh scattering to combustion diagnostics. *Prog Energy Combust Sci.* 1993;19(6):447–485.
11. Miles RB, Lempert WR, Forkey JN. Laser Rayleigh scattering. *Meas Sci Technol.* 2001;12(5):R33–R51.
12. Goldenstein CS, Spearrin RM, Jeffries JB, Hanson RK. Infrared laser-absorption sensing for combustion gases. *Prog Energy Combust Sci.* 2017;60:132–176.
13. Rieker GB, Jeffries JB, Hanson RK. Calibration-free wavelength-modulation spectroscopy for measurements of gas temperature and concentration in harsh environments. *Appl Opt.* 2009;48(29):5546–5560.
14. Liu X, Jeffries JB, Hanson RK. Measurement of non-uniform temperature distributions using line-of-sight absorption spectroscopy. *AIAA J.* 2007;45(2):411–419.
15. Wei C, DI Pineda, Goldenstein CS, Spearrin RM. Tomographic laser absorption imaging of combustion species and temperature in the mid-wave infrared. *Opt Express.* 2018;26(16):20944–20951.
16. Spearrin RM, Ren W, Jeffries JB, Hanson RK. Multi-band infrared CO2 absorption sensor for sensitive temperature and species measurements in high-temperature gases. *Appl Phys B.* 2014;116(4):855–865.
17. Bendana FA, Lee DD, Schumaker SA, Danczyk SA, Spearrin RM. Cross-band infrared laser absorption of carbon monoxide for thermometry and species sensing in high-pressure rocket flows. *Appl Phys B.* 2019;125(11).
18. Cheong KP, Ma L, Wang Z, Ren W. Influence of line pair selection on flame tomography using infrared absorption spectroscopy. *Appl Spectrosc.* 2019;73(5):529–539.
19. Hanson RK, Spearrin RM, Goldenstein CS. *Spectroscopy and Optical Diagnostics for Gases.* Springer; 2016.
20. Gordon IE, Rothman LS, Hill C, et al. The HITRAN2016 molecular spectroscopic database. *J Quant Spectrosc Radiat Transfer.* 2017;203:3–69.
21. Rothman LS, Gordon IE, Barber RJ, et al. HITEMP, the high-temperature molecular spectroscopic database. *J Quant Spectrosc Radiat Transfer.* 2010;111(15):2139–2150.
22. Hui AK, Armstrong BH, Wray AA. Rapid computation of the Voigt and complex error functions. *J Quant Spectrosc Radiat Transfer.* 1978;19(5):509–516.
23. Goldenstein CS, Miller VA, Spearrin R Mitchell, Strand CL. SpectraPlot.com: integrated spectroscopic modeling of atomic and molecular gases. *J Quant Spectrosc Radiat Transfer.* 2017;200:249–257.
24. Liu X, Jeffries JB, Hanson RK, Hinckley KM, MA Woodmansee. Development of a tunable diode laser sensor for measurements of gas turbine exhaust temperature. *Appl Phys B.* 2005;82(3):469–478.
25. Wang Z, Fu P, Hou L, Chao X. Diffuse-reflection-based single-ended laser absorption sensor for H2O temperature and concentration in kerosene-fuelled combustor. *Meas Sci Technol.* 2020;31(10).
26. Zeng H, F Li X Yu, Ou D, Chen L. Measurement of multispecies concentration and gas temperature in an ammonium-dinitramide-based thruster by tunable diode lasers. *Appl Opt.* 2018;57(6):1321–1330.
27. Liu JT, Rieker GB, Jeffries JB, et al. Near-infrared diode laser absorption diagnostic for temperature and water vapor in a scramjet combustor. *Appl Opt.* 2005;44(31):6701–6711.
28. Zhou X, Liu X, Jeffries JB, Hanson RK. Development of a sensor for temperature and water concentration in combustion gases using a single tunable diode laser. *Meas Sci Technol.* 2003;14(8):1459–1468.
29. Farooq A, Jeffries JB, Hanson RK. In situ combustion measurements of H2O and temperature near 2.5 μm using tunable diode laser absorption. *Meas Sci Technol.* 2008;19(7).
30. Ma L, Ning H, Wu J, Ren W. In situ flame temperature measurements using a mid-infrared two-line H2O laser-absorption thermometry. *Combust Sci Technol.* 2017;190(3):393–408.
31. Goldenstein CS, Schultz IA, Spearrin RM, Jeffries JB, Hanson RK. Scanned-wavelength-modulation spectroscopy near 2.5 μm for H2O and temperature in a hydrocarbon-fueled scramjet combustor. *Appl Phys B.* 2014;116(3):717–727.
32. Bryner E, Busa K, Mcdaniel J, Goyne C, Diskin G. In spatially resolved temperature and water vapor concentration distributions in a flat flame burner by tunable diode laser absorption tomography. In: *49th AIAA Aerospace Sciences Meeting Including the New Horizons Forum and Aerospace Exposition.* 2011.
33. Wei C, DI Pineda, Paxton L, Egolfopoulos FN, Spearrin RM. Mid-infrared laser absorption tomography for quantitative 2D thermochemistry measurements in premixed jet flames. *Appl Phys B.* 2018;124(6):1–12.
34. Ma L, Cheong K-P, Ning H, Ren W. An improved study of the uniformity of laminar premixed flames using laser absorption spectroscopy and CFD simulation. *Exp Therm Fluid Sci.* 2020;112.
35. Ma L, Cheong K-P, Yang M, Yuan C, Ren W. On the quantification of boundary layer effects on flame temperature measurements using line-of-sight absorption spectroscopy. *Combust Sci Technol.* 2021:1–18.
36. Zhang G, Liu J, Xu Z, He Y, Kan R. Characterization of temperature non-uniformity over a premixed CH4–air flame based on line-of-sight TDLAS. *Appl Phys B.* 2016;122(1):3.

Kun Duan is a Ph.D. student at the Department of Mechanical and Automation Engineering, The Chinese University of Hong Kong. His current research interest includes combustion diagnostics and trace gas sensing. Email: kduan@mae.cuhk.edu.hk

Da-xin Wen is currently a Research Assistant at the Department of Mechanical and Automation Engineering, The Chinese University of Hong Kong. His research area is combustion diagnostics using laser absorption spectroscopy. Email: dxwen@cuhk.edu.hk

Liu-hao Ma is currently an assistant professor at the Department of Automotive Engineering, Wuhan University of technology. Liu-hao previously worked as a Postdoctoral Fellow and obtained Ph. D. degree at the Department of Mechanical and Automation Engineering at The Chinese University of Hong Kong under the advisory of Prof. Ren Wei. His current research interests focus on high-temperature sensing in harsh environments using novel absorption/dispersion/extinction based techniques, computational fluid dynamics (CFD) simulation of non-reactive and reactive flows and trace gas sensing. Email: liuhaoma@whut.edu.cn